



Cite this: *Dalton Trans.*, 2014, **43**, 16593

Received 16th September 2014,
Accepted 25th September 2014

DOI: 10.1039/c4dt02847c

www.rsc.org/dalton

[Cu(bpy)(P[^]P)]⁺ containing light-emitting electrochemical cells: improving performance through simple substitution[†]

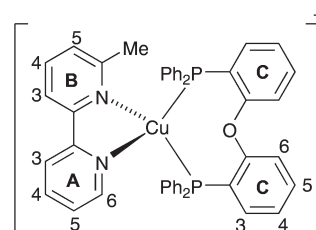
Sarah Keller,^a Edwin C. Constable,^{*a} Catherine E. Housecroft,^a Markus Neuburger,^a Alessandro Prescimone,^a Giulia Longo,^b Antonio Pertegás,^b Michele Sessolo^b and Henk J. Bolink^{*b,c}

Light-emitting electrochemical cells (LECs) containing [Cu(POP)(N[^]N)]⁺[PF₆]⁻ (POP = bis(2-diphenylphosphinophenyl)ether, N[^]N = 6-methyl- or 6,6'-dimethyl-2,2'-bipyridine) exhibit luminance and efficiency surpassing previous copper(I)-containing LECs.

Next-generation efficient lighting devices must exhibit reduced thermal energy loss, increased lifetimes and utilize sustainable materials. Light-emitting electrochemical cells (LECs) are an emerging technology and, like organic light-emitting diodes (OLEDs), dissipate only a very limited amount of energy as heat.¹ Unlike OLEDs, LECs feature a simple architecture and do not require rigorous sealing to maintain an oxygen-free environment. The emissive component of a LEC is a conjugated light-emitting polymer blended with a salt or an ionic transition metal complex (iTMC), typically an iridium or ruthenium compound.¹ We² and others^{3,4} have demonstrated the use of Earth-abundant copper with LECs incorporating emissive [Cu(N[^]N)(P[^]P)]⁺ or [Cu(P[^]P)₂]⁺ complexes (N[^]N = chelating ligand with a bpy or phen metal-binding domain; P[^]P = chelating bis(phosphino) ligand). Sterically demanding P[^]P ligands lead to enhanced emission,¹ and the complexes [Cu(N[^]N)(POP)]⁺ and [Cu(N[^]N)(xantphos)]⁺ (xantphos = 4,5-bis(diphenylphosphino)-9,9-dimethylxanthene) complexes are particularly interesting.^{5–13} Following from our finding that [Cu(POP)(bpy)]⁺ shows encouraging LEC performance, we now demonstrate that simple structural modification of the bpy ligand leads to improved luminance and efficiency, and compare the emission behaviours of LECs containing

[Cu(POP)(6-Mebpy)]⁺[PF₆]⁻ and [Cu(POP)(6,6'-Me₂bpy)]⁺[PF₆]⁻ (6-Mebpy = 6-methyl-2,2'-bipyridine, 6,6'-Me₂bpy = 6,6'-dimethyl-2,2'-bipyridine). McMillin, Walton and coworkers have previously demonstrated that increased substitution in the 2,9-positions of 1,10-phenanthroline (phen) results in significantly enhanced emission behaviour of [Cu(POP)(phen)]⁺-based complexes.¹⁴

[Cu(POP)(6-Mebpy)]⁺[PF₆]⁻ (Scheme 1) was prepared[†] by sequential treatment² of [Cu(MeCN)₄][PF₆]⁺ with POP and 6-Mebpy. The base peak (*m/z* 771.5) in the electrospray mass spectrum arose from [Cu(POP)(6-Mebpy)]⁺. NMR spectra were recorded in CD₂Cl₂, avoiding MeCN which leads to the formation of [Cu(POP)(MeCN)]⁺.¹⁵ The ³¹P{¹H} NMR spectrum of [Cu(POP)(6-Mebpy)]⁺[PF₆]⁻ shows a septet at δ -144.5 ppm ([PF₆]⁻) and a signal at δ -12.4 ppm (POP). ¹H and ¹³C NMR spectra were assigned by COSY, HMQC, HMBC and NOESY methods. The ¹³C NMR spectrum shows one set of signals for the C rings (Scheme 1) confirming that this unit is C₂-symmetric in solution. The Me group desymmetrizes each PPh₂ unit; one Ph group points towards the Me group, while the other is directed away; this is seen in the ¹³C NMR spectrum with two signals for each of C^{D2}, C^{D3} and C^{D4}; C^{D1} gives one triplet (*J*_{PC} = 17.1 Hz). Fig. S1[†] shows the aromatic region of the ¹H NMR spectrum. Distinction between the two pairs of D rings is especially well defined for the *ortho*-protons (labelled H^{D2} and H^{D2'} in Fig. S1[†]).



Scheme 1 Structure of [Cu(POP)(6-Mebpy)]⁺ with atom numbering for NMR spectroscopic assignment. Ph rings in PPh₂ units are labelled D and D' (see text).

^aDepartment of Chemistry, University of Basel, Spitalstrasse 51, CH4056 Basel, Switzerland. E-mail: edwin.constable@unibas.ch, catherine.housecroft@unibas.ch; Tel: +41 61 267 1008

^bInstituto de Ciencia Molecular, Universidad de Valencia, Catedrático José Beltrán 2, Paterna, E-46980, Spain. E-mail: henk.bolink@uv.es

^cFundació General de la Universitat de Valencia (FGUV), PO Box 22085, Valencia, Spain

[†]Electronic supplementary information (ESI) available: Synthesis, characterization and crystallographic data; Tables S1 and S2; Fig. S1–S6. CCDC 996509 and 1009455. For ESI and crystallographic data in CIF or other electronic format see DOI: 10.1039/c4dt02847c



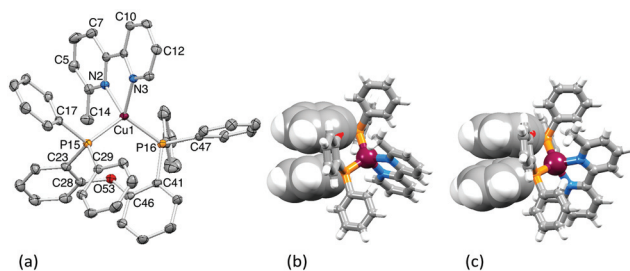


Fig. 1 (a) Structure of the $[\text{Cu}(\text{POP})(6\text{-Mebpy})]^+$ cation (ellipsoids plotted at 40% probability level, H atoms omitted; major occupancy site of 6-Mebpy is shown. Selected bond metrics: Cu1–P15 = 2.2694(4), Cu1–P16 = 2.2514(4), Cu1–N2 = 2.1164(10), Cu1–N3 = 2.0466(10) Å; P15–Cu1–P16 = 112.952(16), P15–Cu1–N2 = 108.81(4), P16–Cu1–N2 = 119.58(4), P15–Cu1–N3 = 113.06(4), P16–Cu1–N3 = 118.09(4), N2–Cu1–N3 = 80.39(4), C28–O53–C46 = 118.79(12)°. Intra-cation stacking of Ph rings in (b) $[\text{Cu}(\text{POP})(6\text{-Mebpy})]^+$ and (c) $[\text{Cu}(\text{POP})(6,6'\text{-Me}_2\text{bpy})]^+$.

$[\text{Cu}(\text{POP})(6,6'\text{-Me}_2\text{bpy})][\text{BF}_4]$ has been reported,¹¹ but for comparison with $[\text{Cu}(\text{POP})(6\text{-Mebpy})][\text{PF}_6]$, we report here $[\text{Cu}(\text{POP})(6,6'\text{-Me}_2\text{bpy})][\text{PF}_6]$.† X-Ray quality crystals of both $[\text{PF}_6]^-$ salts were obtained.† Heavily disordered solvent in the lattice of $[\text{Cu}(\text{POP})(6\text{-Mebpy})][\text{PF}_6]$ necessitated the use of SQUEEZE.¹⁶ Fig. 1a and S2† show the structures of the $[\text{Cu}(\text{POP})(6\text{-Mebpy})]^+$ and $[\text{Cu}(\text{POP})(6,6'\text{-Me}_2\text{bpy})]^+$ cations. In both, atom Cu1 is in a distorted tetrahedral environment. The 6-Mebpy ligand is disordered and modelled over two sites of fractional occupancies 0.925 and 0.075; only the major site is discussed. In $[\text{Cu}(\text{POP})(6\text{-Mebpy})]^+$ the bite-angles of the bpy and POP are 80.39(4)° and 112.952(16)°, respectively, compared to 80.2(2) and 113.36(8)° in $[\text{Cu}(\text{POP})(6,6'\text{-Me}_2\text{bpy})]^+$. The P–Cu–P angles in the methyl derivatives are smaller than in $[\text{Cu}(\text{POP})(\text{bpy})][\text{PF}_6]$ (115.01(2)°),² but the bpy bite angle is unchanged. While the Cu–P distances are similar in $[\text{Cu}(\text{POP})(6\text{-Mebpy})]^+$ and $[\text{Cu}(\text{POP})(\text{bpy})]^+$, the presence of one Me substituent distorts the coordination sphere: Cu1–N2 = 2.1164(10) and Cu1–N3 = 2.0466(10) Å in $[\text{Cu}(\text{POP})(6\text{-Mebpy})]^+$ (Fig. 1) compared to corresponding distances of 2.0480(16) and 2.0738(16) Å in $[\text{Cu}(\text{POP})(\text{bpy})]^+$.² Introducing the Me groups causes significant twisting of the bpy unit coupled with a tilting of the heterocyclic ring plane away from the N–Cu vector (Table S1†). In $[\text{Cu}(\text{POP})(6\text{-Mebpy})]^+$, the phenyl ring containing C29 stacks weakly with that containing C41 (Fig. 1b, angle between ring planes = 18.3°, ring centroid...centroid = 3.86 Å). Despite the greater steric demand of the N[^]N ligand in $[\text{Cu}(\text{POP})(6,6'\text{-Me}_2\text{bpy})]^+$, a weak intra-cation π -stacking interaction is observed (Fig. 1c); angle between ring planes = 17.1° and centroid...centroid separation = 3.78 Å.

The cyclic voltammogram of $[\text{Cu}(\text{POP})(6\text{-Mebpy})][\text{PF}_6]$ (Fig. S3†) shows a reversible $\text{Cu}^+/\text{Cu}^{2+}$ process at +0.69 V (vs. Fc^+/Fc) compared to +0.72 and +0.82 V in $[\text{Cu}(\text{POP})(\text{bpy})][\text{BF}_4]$ and $[\text{Cu}(\text{POP})(6,6'\text{-Me}_2\text{bpy})][\text{BF}_4]$.¹¹ No well-defined reduction processes are observed for $[\text{Cu}(\text{POP})(6\text{-Mebpy})][\text{PF}_6]$ within the solvent accessible window.

The solution absorption spectrum of $[\text{Cu}(\text{POP})(6\text{-Mebpy})][\text{PF}_6]$ (Fig. S4†) exhibits a broad MLCT band at 380 nm (similar

to $[\text{Cu}(\text{POP})(\text{bpy})]^+$, $[\text{Cu}(\text{POP})(6,6'\text{-Me}_2\text{bpy})]^+$, $[\text{Cu}(\text{POP})(\text{phen})]^+$ and $[\text{Cu}(\text{POP})(2,9\text{-Me}_2\text{phen})]^+$ ^{2,5,11} in addition to intense, high energy absorptions from ligand-centred transitions. Photoluminescence (PL) data for PMMA films doped with $[\text{Cu}(\text{POP})(6,6'\text{-Me}_2\text{bpy})][\text{BF}_4]$ have been reported (quantum yield (QY) = 14.5%, lifetime (τ) = 15.7 μs).¹¹ Table 1 summarizes the emission properties of $[\text{Cu}(\text{POP})(6\text{-Mebpy})][\text{PF}_6]$ and $[\text{Cu}(\text{POP})(6,6'\text{-Me}_2\text{bpy})][\text{PF}_6]$ in CH_2Cl_2 solution, PMMA film and solid-state. Excitation of a CH_2Cl_2 solution of $[\text{Cu}(\text{POP})(6\text{-Mebpy})][\text{PF}_6]$ leads to a broad emission (Fig. 2) with a very low QY. This is rationalized in terms of the tetrahedral copper(i) complex undergoing exciplex formation which can occur even with non-coordinating solvents. Since this favours non-radiative relaxation pathways and results in solvent quenching, the emissive properties are better characterized for powder or thin film samples.^{17,18} The PL of both complexes is enhanced in PMMA film† or powdered sample (Table 1). The biexponential fit for the luminescence decay of $[\text{Cu}(\text{POP})(6\text{-Mebpy})][\text{PF}_6]$ is consistent with that of related complexes,^{5,19} and is explained by multiple MLCT transitions at room temperature.¹⁹

Emissions of the complexes in thin PMMA films are blue-shifted with respect to $[\text{Cu}(\text{POP})(\text{bpy})][\text{PF}_6]$ (610 nm, spin-coated film with the same composition as used in LECs) and the QY increased from 2.0%.² The blue-shifting (Fig. 2) on going from solution to PMMA film or solid-state is consistent with similar shifts from 590 to 490 nm, or 536 to 465 nm

Table 1 PL properties of $[\text{Cu}(\text{POP})(\text{N}^{\wedge}\text{N})][\text{PF}_6]$ ($\text{N}^{\wedge}\text{N}$ = 6-Mebpy or 6,6'-Me₂bpy). λ_{exc} = 378 or 372 nm in solution, 365 nm for film and powder

	$[\text{Cu}(\text{POP})(6\text{-Mebpy})][\text{PF}_6]$			$[\text{Cu}(\text{POP})(6,6'\text{-Me}_2\text{bpy})][\text{PF}_6]$		
	$\lambda_{\text{max}}^{\text{em}}/\text{nm}$	QY/%	$\tau_{\text{ave}}^a/\mu\text{s}$	$\lambda_{\text{max}}^{\text{em}}/\text{nm}$	QY/%	$\tau^b/\mu\text{s}$
Solution	610, 639	0.1	—	564, 645sh	—	—
Film	550	10.7	6.0	529	38.4	10.9
Powder	567	9.5	2.6	535	43.2	10.5
Device film	581	5.2	—	557	25.4	—

^a A biexponential fit was used, see Table S1. ^b First order decay.

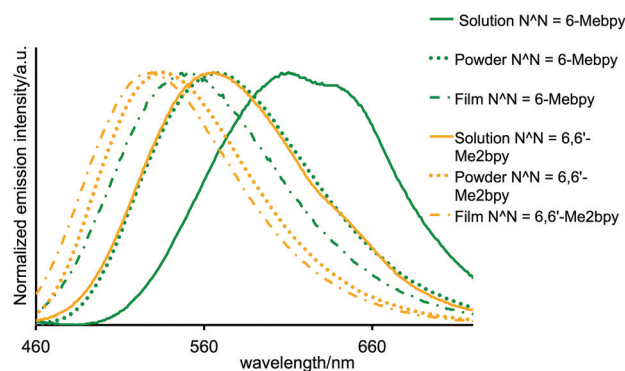


Fig. 2 Normalized PL spectra of $[\text{Cu}(\text{POP})(6\text{-Mebpy})][\text{PF}_6]$ and $[\text{Cu}(\text{POP})(6,6'\text{-Me}_2\text{bpy})][\text{PF}_6]$ in CH_2Cl_2 solutions (2.5×10^{-5} mol dm^{-3} , λ_{exc} = 378 or 372 nm), PMMA thin film (λ_{exc} = 365 nm) and solid state (λ_{exc} = 365 nm).



for $[\text{Cu}(\text{POP})(\text{pypz})]^+$ or $[\text{Cu}(\text{POP})(3\text{-Mepypz})]^+$ (pypz = 2-pyridyl-pyrazole, 3-Mepypz = 3-methyl-2-pyridylpyrazole).⁸

The copper(i) complexes were tested as the active material in LECs. The electroluminescence (EL) of LECs employing $[\text{Cu}(\text{POP})(6\text{-Mebpy})][\text{PF}_6]$ and $[\text{Cu}(\text{POP})(6,6'\text{-Me}_2\text{bpy})][\text{PF}_6]$ shows $\lambda_{\text{max}}^{\text{em}}$ at 574 and 577 nm, respectively (Fig. S5†). These are blue-shifted with respect to the EL of $[\text{Cu}(\text{POP})(\text{bpy})][\text{PF}_6]$ ($\lambda_{\text{max}}^{\text{em}} \approx 597 \text{ nm}$).² The maximum EL emission for $[\text{Cu}(\text{POP})(6,6'\text{-Me}_2\text{bpy})][\text{PF}_6]$ is red-shifted by 20 nm with respect to its PL (557 nm, Table 1), while $[\text{Cu}(\text{POP})(6\text{-Mebpy})][\text{PF}_6]$ shows a blue shift of 7 nm with respect its PL λ_{max} (581 nm, Table 1). LECs were characterized both applying a constant voltage of 4V or a pulsed current of 10 A m^{-2} (50% duty cycle, 1 kHz, block wave). These conditions are similar to those reported for LECs with $[\text{Cu}(\text{POP})(\text{bpy})][\text{PF}_6]$ as the iTMC.² The results from the pulsed current driving are shown in Fig 3. The key parameters of maximum luminance (Lum_{max}), maximum efficacy (Eff_{max}), turn-on time (t_{on}) and lifetime ($t_{1/2}$) are listed in Table 2; t_{on} is defined as the time to reach the Lum_{max} , and $t_{1/2}$ is the time to reach half Lum_{max} .

As expected, the performances of both copper(i)-LECs vary substantially depending on whether they are driven at constant voltage or under pulsed current. However, the device characteristics show the typical low voltage operation that is the hallmark of LECs (Fig. 3). During operation, the ions in the active layer move towards the electrodes, effectively decreasing the

injection barrier and forming p and n doped zones, allowing the LECs to decrease the voltage required to inject electrons and holes independent of the electrode work function.^{20,21} This implies that the time response is strongly influenced by the ionic mobility of the active layer.²²⁻²⁴ Compared to the non-methylated complex $[\text{Cu}(\text{POP})(\text{bpy})][\text{PF}_6]$, devices employing $[\text{Cu}(\text{POP})(6,6'\text{-Me}_2\text{bpy})][\text{PF}_6]$ show a slight reduction of t_{on} at the expense of $t_{1/2}$. This trade-off is typical of LECs, especially when a constant voltage driving mode is used.^{1,25} On the other hand, the maximum luminance of the methyl-substituted complexes (Table 2) is higher than reported for $[\text{Cu}(\text{POP})(\text{bpy})][\text{PF}_6]$.² In general, $[\text{Cu}(\text{POP})(6,6'\text{-Me}_2\text{bpy})][\text{PF}_6]$ showed better performances than $[\text{Cu}(\text{POP})(6\text{-Mebpy})][\text{PF}_6]$, reaching a Lum_{max} of 52 cd m^{-2} by using a pulsed current, with a corresponding Eff_{max} of 5.2 cd A^{-1} . This value is more than three times higher than for $[\text{Cu}(\text{POP})(\text{bpy})][\text{PF}_6]$ ² (1.64 cd A^{-1}) and is consistent with the higher PLQY of $[\text{Cu}(\text{POP})(6,6'\text{-Me}_2\text{bpy})][\text{PF}_6]$ (25.4%) versus 2% for $[\text{Cu}(\text{POP})(\text{bpy})][\text{PF}_6]$. The results demonstrate that a simple modification to the bpy ligand results in noticeably improved LEC luminance and efficiency.

Acknowledgements

We thank the European Research Council (Advanced Grant 267816 LiLo), Swiss National Science Foundation, University of Basel, European Union 7th framework program LUMINET (grant 316906), the Spanish Ministry of Economy and Competitiveness (MINECO) (MAT2011-24594) and the Generalitat Valenciana (Prometeo/2012/053) for support. Ewald Schönhofer prepared 6-Mebpy, and Jonas Schönle assisted with emission measurements. A.P. acknowledges MINECO for an FPI grant.

Notes and references

- R. D. Costa, E. Ortí, H. J. Bolink, F. Monti, G. Accorsi and N. Armaroli, *Angew. Chem., Int. Ed.*, 2012, **51**, 8178.
- R. D. Costa, D. Tordera, E. Ortí, H. J. Bolink, J. Schönle, S. Graber, C. E. Housecroft, E. C. Constable and J. A. Zampese, *J. Mater. Chem.*, 2011, **21**, 16108.
- N. Armaroli, G. Accorsi, M. Holler, O. Moudam, J. F. Nierengarten, Z. Zhou, R. T. Wegh and R. Welter, *Adv. Mater.*, 2006, **18**, 1313.
- O. Moudam, A. Kaeser, B. Delavaux-Nicot, C. Duhayon, M. Holler, G. Accorsi, N. Armaroli, I. Seguy, J. Navarro, P. Destruel and J. F. Nierengarten, *Chem. Commun.*, 2007, 3077.
- K. Zhang and D. Zhang, *Spectrochim. Acta, Part A*, 2013, **124**, 341.
- L. Bergmann, J. Friedrichs, M. Mydlak, T. Baumann, M. Nieger and S. Bräse, *Chem. Commun.*, 2013, **49**, 6501.

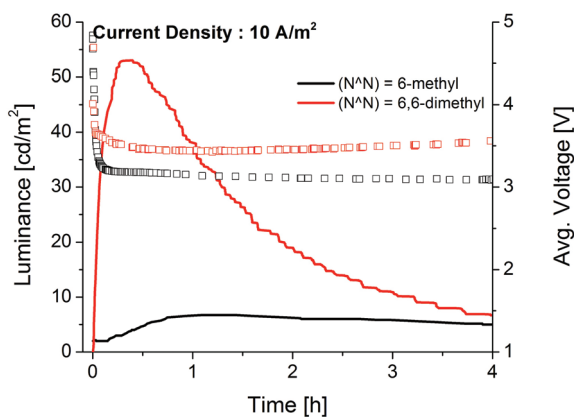


Fig. 3 Luminance (solid line) and voltage (open squares) for ITO/PEDOT:PSS/iTMC:[Emim][PF₆] 1:1/AI LECs measured at a pulsed current driving (avg. current 10 A m^{-2} , 50% duty cycle, 1 kHz, block wave).

Table 2 Performance for ITO/PEDOT:PSS/iTMC:[Emim][PF₆] 1:1/AI LECs based on the copper(i) complexes at constant voltage (DC 4V) and pulsed current (avg. current density 10 A m^{-2} , 50% duty cycle, 1 kHz, block wave)

Complex	Driving mode	$\text{Lum}_{\text{max}}/\text{cd m}^{-2}$	$\text{Eff}_{\text{max}}/\text{cd A}^{-1}$	t_{on}/h	$t_{1/2}/\text{h}$
$[\text{Cu}(\text{POP})(6\text{-Mebpy})][\text{PF}_6]$	DC 4V	14.4	0.1	0.15	0.58
	PC 10 A m^{-2}	6.7	0.6	1.09	11.5
$[\text{Cu}(\text{POP})(6,6'\text{-Me}_2\text{bpy})][\text{PF}_6]$	DC 4V	11.2	3.0	0.35	1.05
	PC 10 A m^{-2}	53.0	5.2	0.39	1.47



- 7 E. Mejía, S.-P. Luo, M. Karnahl, A. Friedrich, S. Tschierlei, A.-E. Surkus, H. Junge, S. Gladiali, S. Lochbrunner and M. Beller, *Chem. – Eur. J.*, 2013, **19**, 15972.
- 8 X.-L. Chen, R. Yu, Q.-K. Zhang, L.-J. Zhou, X.-Y. Wu, Q. Zhang and C.-Z. Lu, *Chem. Mater.*, 2013, **25**, 3910.
- 9 A. Kaeser, M. Mohankumar, J. Mohanraj, F. Monti, M. Holler, J.-J. Cid, O. Moudam, I. Nierengarten, L. Karmazin-Brelot, C. Duhayon, B. Delavaux-Nicot, N. Armaroli and J.-F. Nierengarten, *Inorg. Chem.*, 2013, **52**, 12140.
- 10 C. Femoni, S. Muzzioli, A. Palazzi, S. Stagni, S. Zacchini, F. Monti, G. Accorsi, M. Bolognesi, N. Armaroli, M. Massi, G. Valenti and M. Marcaccio, *Dalton Trans.*, 2013, **42**, 997.
- 11 I. Andrés-Tomé, J. Fyson, F. Baiao Dias, A. P. Monkman, G. Iacobellis and P. Coppo, *Dalton Trans.*, 2012, **41**, 8669.
- 12 C. L. Linfoot, M. J. Leidl, P. Richardson, A. F. Rausch, O. Chepelin, F. J. White, H. Yersin and N. Robertson, *Inorg. Chem.*, 2014, DOI: 10.1021/ic500889s.
- 13 S.-M. Kuang, D. G. Cuttall, D. R. McMillin, P. E. Fanwick and R. A. Walton, *Inorg. Chem.*, 2002, **41**, 3313.
- 14 D. G. Cuttall, S.-M. Kuang, P. E. Fanwick, D. R. McMillin and R. A. Walton, *J. Am. Chem. Soc.*, 2002, **124**, 6.
- 15 J. Yuasa, M. Dan and T. Kawai, *Dalton Trans.*, 2013, **42**, 16096.
- 16 A. L. Spek, *Acta Crystallogr., Sect. D: Biol. Crystallogr.*, 2009, **65**, 148.
- 17 N. A. Gothard, M. W. Mara, J. Huang, J. M. Szarko, B. Rolczynski, J. V. Lockard and L. X. Chen, *J. Phys. Chem. A*, 2012, **116**, 1984.
- 18 N. Armaroli, G. Accorsi, F. Cardinali and A. Listorti, *Top. Curr. Chem.*, 2007, **280**, 69.
- 19 J.-J. Cid, J. Mohanraj, M. Mohankumar, M. Holler, G. Accorsi, L. Brelot, I. Nierengarten, O. Moudam, A. Kaeser, B. Delavaux-Nicot, N. Armaroli and J.-F. Nierengarten, *Chem. Commun.*, 2013, **49**, 859.
- 20 S. van Reenen, P. Matyba, A. Dzwilewski, R. A. J. Janssen, L. Edman and M. Kemerink, *J. Am. Chem. Soc.*, 2010, **132**, 13776.
- 21 M. Lenes, G. Garcia-Belmonte, D. Tordera, A. Pertegás, J. Bisquert and H. J. Bolink, *Adv. Funct. Mater.*, 2011, **21**, 1581.
- 22 S. van Reenen, P. Matyba, A. Dzwilewski, R. A. J. Janssen, L. Edman and M. Kemerink, *Adv. Funct. Mater.*, 2011, **21**, 1795.
- 23 R. D. Costa, A. Pertegás, E. Ortí and H. J. Bolink, *Chem. Mater.*, 2010, **22**, 1288.
- 24 Y. Shen, D. D. Kuddes, C. A. Naquin, T. W. Hesterberg, C. Kusmierz, B. J. Holliday and J. D. Slinker, *Appl. Phys. Lett.*, 2013, **102**, 203305.
- 25 T. Hu, L. He, L. Duan and Y. Qiu, *J. Mater. Chem.*, 2012, **22**, 4206.

